半 导 体 学 报
CHINESE JOURNAL OF SEMICONDUCTORS

A New Method for InGaAs/InP Composite Channel HEMTs Simulation*

Liu Liang†, Zhang Haiying, Yin Junjian, Li Xiao, Xu Jingbo, Song Yuzhu, and Liu Xunchun

(*Institute of Microelectronics, Chinese Academy of Sciences, Beijing 100029, China*)

Abstract: A new method is used to simulate InGaAs/InP composite channel high electron mobility transistors (HEMTs). By coupling the hydrodynamic model and the density gradient model, the electron density distribution in the channel in different electric fields is obtained. This method is faster and more robust than traditional methods and should be applicable to other types of HEMTs simulations. A detailed study of the InGaAs/InP composite channel HEMTs is presented with the help of simulations.

Key words: InP; InGaAs; composite channel; HEMTs; simulation

EEACC: 2520; 2560

CLC number: TN302 **Document code**: A **Article ID**: 0253-4177(2007)11-1706-06

1 Introduction

InP-based high electron mobility transistors (HEMTs) have demonstrated excellent high-frequency and low-noise performance at millimeter-wave frequencies. However, the enhanced impact-ionization effects, which take place in the narrow-bandgap InGaAs channel, make the breakdown voltages of InP HEMTs too low. Thus, the application of these devices to power millimeter-wave systems is limited[1].

To enhance the breakdown voltage, Enoki[2] proposed an InGaAs/InP composite channel. Since then, a series of studies on composite channel HEMT have been reported[3~6]. However, most of them focused on experiments, while few explored computations or simulations. In some studies, computations by self-consistently solving Poisson's and Schrödinger's equations were used to simulate composite channel HEMTs[2,4]. However, simulations with this method tend to be slow and often lead to convergence problems.

In this paper, a new method is proposed to simulate the InGaAs/InP composite channel HEMT, i. e., coupling the hydrodynamic model and the density gradient model to compute the electron density distribution in the channel in different electric fields of the devices. This method is numerically robust and significantly faster than solving Schrödinger's equations, and should be applicable to other HEMT devices. In our simulation, we focus on the electron density distribution in the channel in different electric fields to help improve the designs of the composite channel epitaxial layer structure and the device structure. A detailed study of the InGaAs/InP composite channel HEMTs is presented. With the help of simulations, an InGaAs/InP composite channel HEMTs epitaxial layer is designed, and HEMTs devices with 5.9V on-state breakdown voltage are fabricated on this epitaxial layer.

2 Model description

In our simulations, a hydrodynamic model (HD) is used as the transport equation, and a density gradient model (DG) is used to describe the quantum effect. The platform for the simulations is the multidimensional device simulator Sentaurus Device from Synopsys. The main feature of our simulations is to couple the hydrodynamic model and the density gradient model to solve the equations and obtain physical quantity. Simulations with this method become numerically robust and significantly faster than simulations using tradi-

* Project supported by the State Key Development Program for Basic Research of China (No. G2002CB311901)

† Corresponding author. Email: liuliang@ime.ac.cn

Received 28 May 2007, revised manuscript received 20 June 2007

©2007 Chinese Institute of Electronics

tional methods. Before proceeding, we will introduce these two models.

2.1 Hydrodynamic model

With continued scaling into the deep submicron regime, characteristics of semiconductor devices cannot be properly described using the conventional drift-diffusion transport model. In particular, the drift-diffusion (DD) approach cannot reproduce velocity overshoot and often overestimates the impact ionization generation rates. The Monte Carlo (MC) method for the solution of the Boltzmann kinetic equation presents one alternative, but its computational expense along with the related statistical uncertainty often make MC impractical for the simulation of the devices. In this case, the hydrodynamic (or energy balance) model provides a very good compromise.

Since the work of Stratton[7] and Bløtekjær[8], there have been many variations of this model[9~11]. In general, the model implemented in Sentaurus consists of the basic semiconductor equations and the energy conservation equations for the electrons, holes, and the lattice. The basic semiconductor equations, which include the Poisson equation (Eq. (1)) and continuity equations (Eqs. (2,3)), are written as

$$\nabla \varepsilon \cdot \nabla \Psi = -q(p - n + N_{D^+} - N_{A^-}) \quad (1)$$

$$\nabla \cdot \boldsymbol{J}_n = qR + q\frac{\partial n}{\partial t} \quad (2)$$

$$-\nabla \cdot \boldsymbol{J}_p = qR + q\frac{\partial p}{\partial t} \quad (3)$$

where ε is the electrical permittivity, Ψ is the electrostatic potential, q is the elementary electronic charge, n and p are the electron and hole densities, N_{D^+} and N_{A^-} are the number of ionized donors and acceptors, $\boldsymbol{J}_n$ is the electron current density, $\boldsymbol{J}_p$ is the hole current density, and R is the net electron-hole recombination rate.

The energy conservation equations are written as

$$\frac{\partial W_n}{\partial t} + \nabla \cdot \boldsymbol{S}_n = \boldsymbol{J}_n \cdot \nabla E_C + \frac{dW_n}{dt}\Big|_{coll} \quad (4)$$

$$\frac{\partial W_p}{\partial t} + \nabla \cdot \boldsymbol{S}_p = \boldsymbol{J}_p \cdot \nabla E_V + \frac{dW_p}{dt}\Big|_{coll} \quad (5)$$

$$\frac{\partial W_L}{\partial t} + \nabla \cdot \boldsymbol{S}_L = \frac{dW_L}{dt}\Big|_{coll} \quad (6)$$

where W_n, W_p, W_L are respectively the energy densities of the electrons, holes, and the lattice, and $\boldsymbol{S}_n$, $\boldsymbol{S}_p$, $\boldsymbol{S}_L$ are respectively the energy fluxes of the electrons, holes, and the lattice. In the hydrodynamic model, the carrier temperatures T_n and T_p are assumed to be unequal to the lattice temperature T_L. The temperatures and some other physics characteristics can be obtained by solving the equations in the model. More details of the hydrodynamic model are seen in Refs. [7~12].

2.2 Density gradient model

HEMTs use the high mobility and high velocity of the two-dimensional electron gas (2DEG) formed at the heterointerface. The electron motion in the 2DEG is quantized in the direction perpendicular to the heterointerface because the de Broglie wavelength is larger than the width of the potential well (the de Broglie wavelength of a thermal electron is approximately 26nm at room temperature and longer at lower temperature)[13]. Therefore, the quantization effects should be taken into consideration. To include the quantization effects in a device simulation, a precise method is solving the Schrödinger equation, but it will make the computation very slow and often lead to convergence problems. A simple approach is to introduce an additional potential, such as quantity Λ, into the classical electron density formula, as

$$n = N_C \exp\left(\frac{E_{F_n} - E_C - \Lambda}{kT}\right) \quad (7)$$

where T is the carrier temperature, k is the Boltzmann constant, N_C is the conduction band density-of-states, E_C is the conduction band energy, and E_{F_n} is the electron Fermi energy. The most important effects related to the density modification (due to quantization) can be captured by proper models for Λ.

For the density gradient model[14,15], Λ in Eq. (7) is given by a partial differential equation:

$$\Lambda = -\frac{\gamma\hbar^2}{12m}\left\{\nabla^2 \lg n + \frac{1}{2}(\nabla \lg n)^2\right\} = -\frac{\gamma\hbar^2}{6m} \times \frac{\nabla^2\sqrt{n}}{\sqrt{n}} \quad (8)$$

where $\hbar = h/2\pi$ is the reduced Planck constant, m is the density-of-states (DOS) mass, and γ is a fit factor.

We use the hydrodynamic model as the transport equation and the DG model to describe the quantum effect in the simulation. Coupling these two models, the simulation is numerically robust and significantly faster than using traditional

Table 1 Composite channel HEMT epitaxial layer structure

InAlAs/InGaAs/InP HEMT structure			
Layer	Thickness/nm	Dopant	Concentration
$In_{0.53}Ga_{0.47}As$	10	Si	$5\times10^{18}cm^{-3}$
InP	6		
$In_{0.52}Al_{0.48}As$	10		
Si delta doped layer		Si	$4\times10^{12}cm^{-2}$
$In_{0.52}Al_{0.48}As$	4		
$In_{0.53}Ga_{0.47}As$	6		
InP	5		
InP	8	Si	$2\times10^{18}cm^{-3}$
$In_{0.52}Al_{0.48}As$ buffer	300		
SI InP substrate (100)			

methods.

3 Device simulation

The composite-channel HEMT epitaxial layer structure we designed is shown in Table 1. It consists of an InGaAs cap layer (10nm), an InP etch stopper layer (6nm), an InAlAs barrier layer (10nm), a Si delta doped layer, an InAlAs spacer layer (4nm), a composite channel (19nm), and a InAlAs buffer (300nm). The composite-channel consists of a lattice-matched InGaAs channel (6nm), an undoped InP (5nm) channel, and a uniformly n-doped InP layer (8nm, $2\times10^{18}cm^{-3}$). A 5nm-thick undoped InP was inserted between the InGaAs channel and the n-InP subchannel to avoid Si diffusion into the InGaAs channel. The n-doped InP layer acts as a carrier supply layer as well as a channel, so the electrons in the InGaAs are supplied from both the delta doped layer and the n-InP layer.

The gate length of the device in the simulation is 0.3μm. The spacing between the source and drain electrode pads is 2μm. The Schottky barrier height of $\phi_B=0.35V$ is estimated based upon experimental observation. Important model parameters for GaAs, InAs, AlAs, and InP such as energy band structure and energy relaxation time were based on Refs. [12, 13, 16]. Linear interpolations were adopted to compute parameter values as a function of the mole fraction in InGaAs and InAlAs. Table 2 summarizes some important parameter values adopted in the simulations. The other parameters of the hydrodynamic and DG models were set as their default values in Sentaurus for the different materials.

Table 2 Some important parameter values adopted in the simulation

	InAs	GaAs	AlAs	InP
Dielectric constant	14.55	13.18	10.06	12.40
Band gap energy at 0K/eV	0.411	1.519	2.230	1.421
Electron affinity/eV	4.9	4.1	3.5	4.4
Effective conduction band density of states at $T=300K$ /cm^{-3}	8.72×10^{16}	4.42×10^{17}	1.1100×10^{18}	5.6600×10^{17}
Energy relaxation time/ps	1.0	1.0	1.0	1.0

In the simulation, we focus on the electrical field distribution and the electron density distribution in the channel, because it is helpful for studies on the composite channel HEMT and to improve the epitaxial layer design.

4 Simulation results and discussion

Figure 1 shows a vertical cross section of the electric field distribution under the gate at zero and the drain at 1V bias as predicted by the simulations. Figure 2 shows the electric field distribution in a vertical cross section under the gate at zero and the drain at 3V bias as predicted by the simulations. From the electric field distribution cross section, it can be observed that the electric field in the region near the source is low and, in the region near the drain, it becomes higher. Comparing Fig. 1 with Fig. 2, it can be observed that the electric field of each point near the gate at $V_d=3V$ is higher than it is at $V_d=1V$ under the same gate bias.

Figure 3 (a) shows the simulations results of the band structure and electron density distribution along a vertical cross section at the source

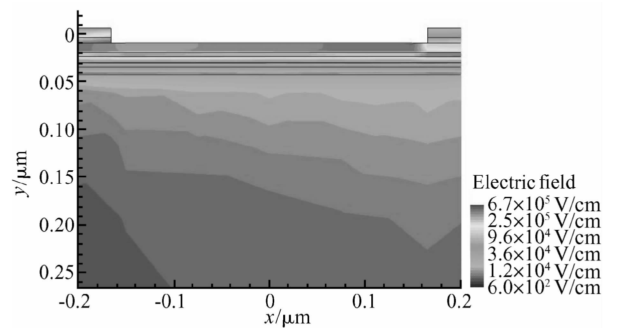

Fig. 1 Electric field distribution in a vertical cross section under the gate at zero and the drain at 1V bias as predicted by the simulations

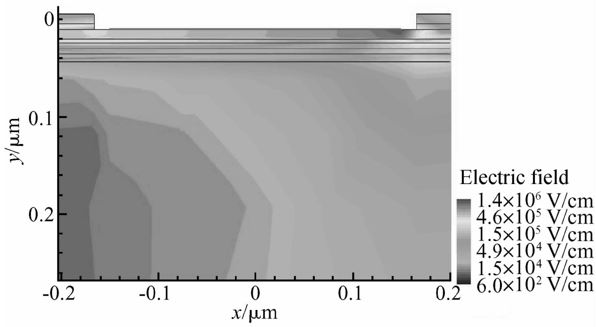

Fig. 2 Electric field distribution in a vertical cross section under the gate at zero and the drain at 3V bias as predicted by the simulations

side of the gate under the gate at zero and drain at 1V bias, where y is the direction perpendicular to the heterointerface. As it shows, at the source side, where the electric field is low, electrons exist mainly in the InGaAs channel (the band gap energy is low). Figure 3 (b) shows the simulations results of the band structure and electron density distribution along a vertical cross section at the

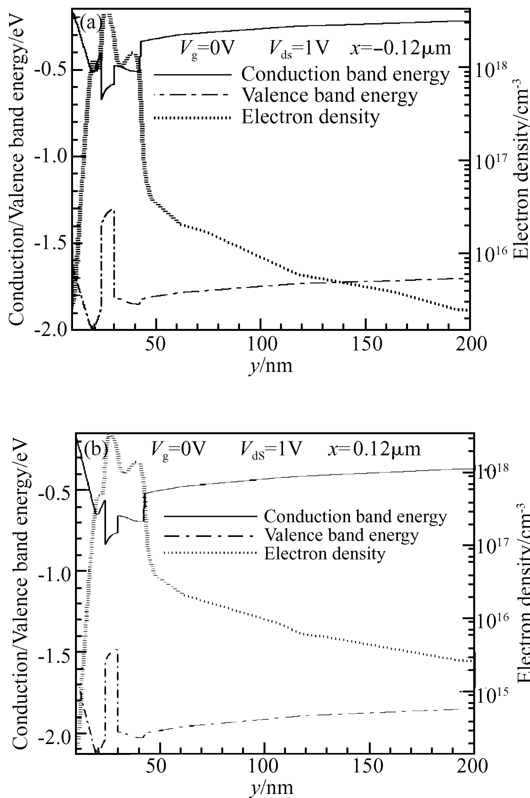

Fig. 3 Simulations results of the band structure and electron density distribution along a vertical cross section under the gate at zero and drain at 1V bias (a) On the source side of the gate; (b) On the drain side of the gate

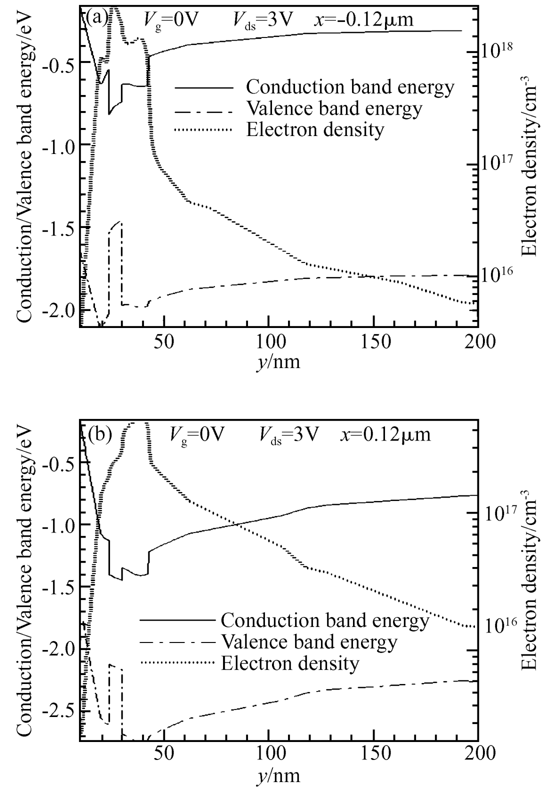

Fig. 4 Simulations results of the band structure and electron density distribution along a vertical cross section under the gate at zero and drain at 3V bias (a) On the source side of the gate; (b) On the drain side of the gate

drain side of the gate under the gate at zero and drain at 1V bias. As it shows, on the drain side, where the electric field strength is not high enough, the electrons exist mainly in the InGaAs channel (the band gap energy is high). Compared with Fig. 3 (a), Figure 3 (b) shows a higher percentage of the electron distribution in the InP channel. This is because the electric field strength at the drain is higher than it is at the source side. As the drain voltage increases to 3V, at the source side, where the electric field still low, electrons still exist mainly in the InGaAs channel as Figure 4(a) shows. Since the electric field at $V_d = 3V$ is higher than $V_d = 1V$ at each point near the gate as mentioned above, some electrons transfer into the InP channel, so the electron density in the InGaAs channel at the source side is lower at $V_d = 3V$ (Fig. 4(a)) than it is at $V_d = 1V$ (Fig. 3 (a)). At the drain side when $V_d = 3V$, the electric field strength is very high, almost all electrons exist in the InP channel as Figure 4 (b) shows. Since the drift velocity of the electrons on the drain side of

the gate is higher than on the source side, the electron density on the drain side is lower than that on the source side, due to current continuity.

The electron densities of our simulations have the same orders with the results in Ref. [4], which were obtained by self-consistently solving Poisson's and Schrödinger's equations. But our method is faster and more robust. As some models for compound semiconductors material are not accurate and some practical matters in device fabrication are not take into account, it may affect the precision of the simulations results. But it is not a big problem for us to predict the devices' behaviors.

The mobility of electrons in InGaAs at the low electric field is high, but its threshold energy (0.92eV) for impact-ionization is low, which is why the breakdown voltage of traditional InGaAs channel HEMTs is low. InP has a high drift velocity in high electrical fields and its threshold energy for impact ionization (1.69eV) is high. Thus from the simulation results it is easy to understand that the composite-channel structure can use both the high mobility of electrons in InGaAs in the low electric field and the high drift velocity and low impact ionization coefficients in InP in the high electric field. With the composite-channel structure, HEMTs' breakdown voltage will be increased. To verify the conclusion, using the same eptaxial layer structure in the simulation, HEMTs with 5.9V on-state breakdown voltage are fabricated. The on-state breakdown curve is shown in Fig. 5. Compared with traditional InGaAs channel HEMTs, the breakdown voltage has improved greatly (The on-state breakdown voltage of traditional InGaAs channel HEMTs with the same device structure is about 2V.).

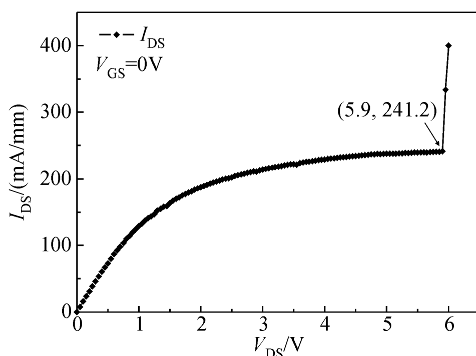

Fig. 5 On-state breakdown characteristic of the composite-channel HEMTs

5 Conclusions

A InGaAs/InP composite channel HEMT is simulated by coupling the hydrodynamic model and the density gradient model. This new simulation method is numerically robust and significantly faster than traditional methods and should be applicable to other HEMT devices. According to the simulations, it is easy to understand that the composite-channel structure can use both the high mobility of electrons in InGaAs in the low electric field and the high drift velocity and low impact ionization coefficients in InP in the high electric field. HEMTs' breakdown voltage can be increased greatly using a composite-channel structure. To verify the conclusion, composite-channel HEMTs with 5.9V on-state breakdown voltage were fabricated.

References

[1] Chevalier P, Wallart X, Mollot F, et al. Composite channel HEMTs for millimeter-wave power applications. 10th International Conference on Indium Phosphide and Related Materials, 1998, 11～15: 207

[2] Enoki T, Arai K, Kohzen A, et al. InGaAs/InP double channel HEMT on InP. 4th International Conference on Indium Phosphide and Related Materials, 1992, 21～24: 14

[3] Matloubian M, Liu T, Jelloian L M, et al. K-band GaInAs/Inp channel power HEMTs. Electron Lett, 1995, 31(9): 761

[4] Enoki T, Arai K, Kohzen A, et al. Design and characteristics of InGaAs/InP composite-channel HFET's. IEEE Trans Electron Devices, 1995, 42(8): 1413

[5] Meneghesso G, Neviani A, Oesterholt R, et al. On-state and off-state breakdown in GaInAs/InP composite-channel HEMT's with variable GaInAs channel thickness. IEEE Trans Electron Devices, 1999, 46(1): 2

[6] Boudrissa M, Delos E, Wallaert X, et al. A 60GHz high power composite channel GaInAs/InP HEMT on InP substrate with $L_G = 0.15\mu$m. 13th International Conference on Indium Phosphide and Related Materials, 2001, 14～18: 196

[7] Stratton R. Diffusion of hot and cold electrons in semiconductor barrier. Phys Rev, 1962, 126(6): 2002

[8] Bløtekjær K. Transport equations for electrons in two-valley semiconductors. IEEE Trans Electron Devices, 1970, ED-17 (1): 38

[9] Benvenuti A, Bonani F, Ghione G, et al. Analysis of output NDR in power AlGaAs/GaAs HBTs by means of a thermalfully hydrodynamic model. International Semiconductor Device Research Symposium, 1993, 2: 499

[10] Szeto S, Reif R. A unified electrothermal hot-carrier transport model for silicon bipolar transistor simulation. Solid-State Electron, 1989, 32(4): 307

[11] Apanovich Y, Lyumkis E, Polsky B, et al. Steady-state and transient analysis of submicron devices using energy balance

and simplified hydrodynamic models. IEEE Trans CAD, 1994, 13: 702
[12] Synopsys. Sentaurus Device Manual. 2005
[13] Shur M. GaAs device and circuits. New York: Plenum Press, 1987
[14] Ancona M G, Tiersten H F. Macroscopic physics of the silicon inversion layer. Phys Rev B, 1987, 35(15): 7959
[15] Ancona M G, Iafrate G J. Quantum correction to the equation of state of an electron gas in a semiconductor. Phys Rev B, 1989, 39(13): 9536
[16] Sze S M. Modern semiconductor device physics. New York: John Wiley & Sons, 1997

一种 InGaAs/InP 复合沟道高电子迁移率晶体管模拟的新方法*

刘　亮† 张海英　尹军舰　李　潇　徐静波　宋雨竹　刘训春

（中国科学院微电子研究所，北京　100029）

摘要：采用一种新方法对 InGaAs/InP 复合沟道高电子迁移率晶体管进行了模拟.该方法通过流体力学模型和密度梯度模型的联合求解,得到了沟道内的电子密度分布.与一些传统方法相比,该方法收敛性更好,速度更快,且同样适用于其他类型高电子迁移率晶体管器件的模拟.利用仿真对 InGaAs/InP 复合沟道高电子迁移率晶体管进行了深入研究.

关键词：InP；InGaAs/InP；复合沟道；高电子迁移率晶体管；模拟
EEACC：2520；2560
中图分类号：TN302　　**文献标识码**：A　　**文章编号**：0253-4177(2007)11-1706-06

* 国家重点基础研究发展规划资助项目(批准号:G2002CB311901)
† 通信作者.Email:liuliang@ime.ac.cn
2007-05-28 收到,2007-06-20 定稿
©2007 中国电子学会